Polymer Bulletin
https://doi.org/10.1007/s00289-024-05471-y

ORIGINAL PAPER

Study of the effect of hexagonal boron nitride addition to thermoplastic polyester elastomer composites reinforced with carbon, glass and basalt fibers

Okan Gul[1] · Nevin Gamze Karsli[2] · Cihat Gul[3] · Ali Durmus[4] · Taner Yilmaz[1]

Received: 14 May 2024 / Revised: 13 August 2024 / Accepted: 21 August 2024

Abstract

In this study, the effect of hexagonal boron nitride (hBN) addition at different weight ratios to thermoplastic polyester elastomer (TPEE) reinforced with three different fiber types, namely carbon fiber (CF), glass fiber (GF) and basalt fiber (BF), on the mechanical, tribological and thermal properties of the composites was investigated. Adhesive wear test for tribological analysis, tensile and three-point bending tests for mechanical analysis, differential scanning calorimetry and thermogravimetric analyses for thermal investigation and scanning electron microscopy analysis for morphological evaluation were applied. The results showed that the addition of hBN to fiber-reinforced TPEE composites, regardless of the fiber type, and the increasing weight ratio of hBN improved the wear, mechanical and thermal properties of the composites. However, when comparing the synergistic effect of hBN when used simultaneously with fiber reinforcement on the basis of fiber type, CF was found to outperform GF and BF fiber types and hybrid reinforced composites containing 10 wt% hBN and CF to exhibit superior tribological, mechanical and thermal properties. It is also concluded that BF performs at a comparable level to GF and therefore can be used instead of GF in some applications.

✉ Nevin Gamze Karsli
ngkarsli@gmail.com; gamze.karsli@kocaeli.edu.tr

[1] Department of Mechanical Engineering, Kocaeli University, 41380 Kocaeli, Turkey

[2] Present Address: Department of Aviation and Aerospace Engineering, Kocaeli University, 41380 Kocaeli, Turkey

[3] Research & Development Department, Valeo Otomotiv San.Ve Tic. A.Ş, 16245 Bursa, Turkey

[4] Department of Mechanical Engineering, Bursa Uludağ University, 16059 Bursa, Turkey

Published online: 28 August 2024

Graphical abstract

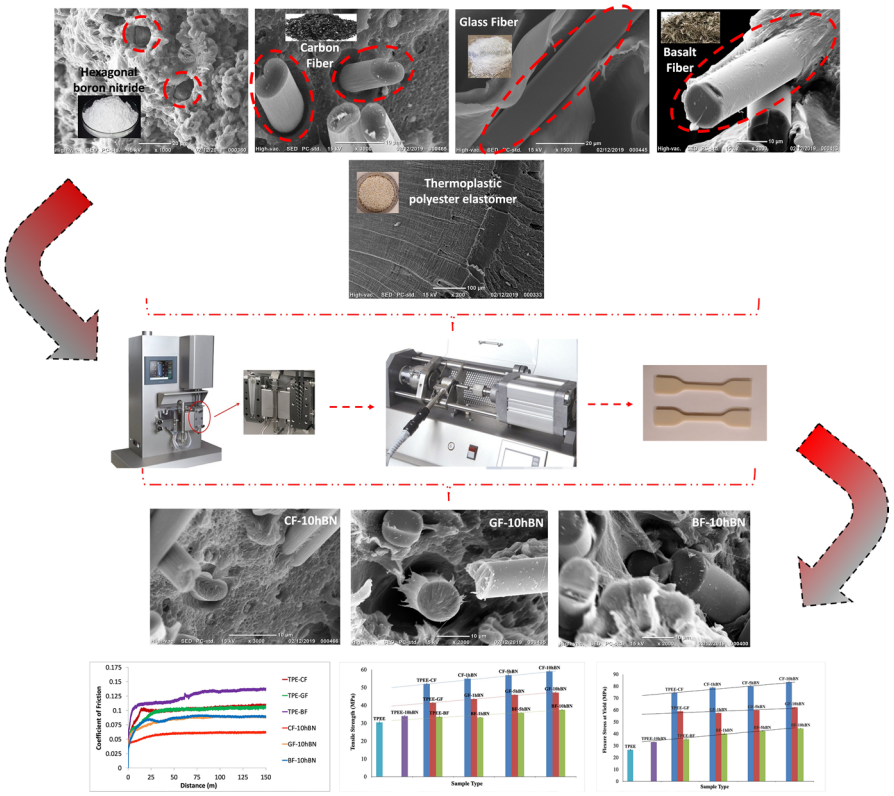

Keywords Hexagonal boron nitride · Thermoplastic polyester elastomer · Carbon fiber · Glass fiber · Basalt fiber

Introduction

Thermoplastic elastomers (TPEs), which are block copolymers, are consisting of hard crystalline and soft amorphous segments, combining the physical properties of elastomers with the easy processability and good strength of thermoplastics. Soft amorphous segments provide flexibility, and hard crystalline segments provide thermal and mechanical strength. The final properties of TPEs are determined by the ratio between hard and soft segments and the segment composition. DuPont™ has developed a new type of thermoplastic polyester elastomer (TPEE) branded Hytrel®. Hytrel® has a polybutylene terephthalate structure as the hard crystalline segment and a polyether structure as the soft amorphous segment. Hytrel® is a type of polymer extensively used in many fields, especially in the automotive industry, and was chosen as the matrix material in this study [1–6].

Development of polymer matrix composites is very common where there is a need for high-performance materials. However, high performance cannot be achieved with a single polymer. Therefore, polymer modification methods such as copolymerization, reinforcement and blending are used. Among these methods, polymer reinforcement stands out as a relatively simple process that offers limitless opportunities to create materials with improved performance. A widely used method to improve mechanical, tribological and thermal properties and to extend the application range of polymeric materials is the incorporation of fillers in the form of fibers and/or particles. Carbon fibers, glass fibers, carbon nanotubes, graphene, boron nitride, layered silicates and others have been used as fillers to reinforce TPEE [1–16]. The short fiber reinforcement provides performance between that of conventional continuous fiber-reinforced composites and that of unreinforced polymer. Owing to their exceptional characteristics including high thermal resistance and mechanical strength, low density, good wear resistance, etc., carbon fiber (CF) and glass fiber (GF) are promising materials for short fiber reinforcement of polymer matrix [17–19]. However, few studies in the literature have examined the influence of the use of short CF and GF in TPEE on the thermal, tribological and mechanical properties of the material [2, 7, 18]. On the other hand, in the production of TPEE matrix composites, basalt fiber (BF) is emerging as an alternative fiber type to CF and GF. Although production of BF is similar to that of GF, BF requires less energy and contains no additives. As a result, BF is less expensive to produce than glass or carbon fiber. BF has mechanical properties similar to those of GF. In addition, it has advantages such as non-flammability, high chemical resistance and thermal resistance. This makes BF a good alternative to GF for the reinforcement of composites used in a number of industries, including marine, automotive and construction. Specifically, the large number of micropores in its structure contributes to its thermal insulation and flame retardancy [20]. Despite all these advantages, the applications of BF with thermoplastic matrices remain extremely limited, and there are even no studies reported in the literature on the production of TPEE matrix composites [20–22].

The addition of particles to the neat polymer matrix or fiber-reinforced composites is another method used to further enhance the properties of polymeric materials [2–6, 13, 14, 18]. However, the shape, size distribution, surface area and chemistry of the particles added to the material strongly influence its behavior [2, 5]. For example, platelet-shaped nanoparticles represent a special class of reinforcement for polymers and, if properly oriented in the polymer matrix, can provide a significant extent of reinforcement [3, 5, 13]. Carbon nanotubes, graphene nanoplatelets, graphene oxide, mica, fly ash, nanosilica and boron nitride are some of the nanoparticle types commonly used in TPEEs [1–6, 13–15, 18]. Suresha et al. examined the influence of graphene nanoplatelets (GnPs) on the mechanical and the physical properties of short CF-reinforced polyamide 66/thermoplastic copolyester elastomer composites and found that the addition of GnPs improved the tensile properties [18].

In addition to these types of fillers, the hexagonal boron nitride (hBN) nanomaterial is of great interest as a functional filler for the modification and reinforcement of the polymeric materials. Also known as white graphite, hBN's hexagonal layered structure of covalently bonded B–N atoms is similar to graphite. Widely used as an

electrical insulator and thermal conductor, it is chemically and thermally stable [23]. Due to its layered form and the low Van der Waals forces between the layers, it is also used as a solid lubricant [24, 25].

To the knowledge of the authors, there are no studies that have investigated hBN as a platelet-shaped nanoparticle reinforcement for neat TPEE matrix or fiber/matrix material compositions, although one study has been reported that investigated the influence of boron nitride incorporation on the thermal expansion behavior of Hytrel® [13].

Therefore, further studies on the tribological, thermal and mechanical performance of both TPEE matrix composites reinforced with different types of fibers and hybrid composites simultaneously reinforced with hBN and fibers are needed. Therefore, the effect of the addition of hBN at different weight ratios to TPEE matrix reinforced with three different fiber types, CF, GF and BF, on the thermal, tribological and mechanical performance has been studied.

Materials and method

Materials

TPEE was supplied from DuPont™ with the brand name "Hytrel® 7246" (Form: pellet, density: 1.26 g/cm^3, melting temperature: 218 °C, glass transition temperature: 25 °C). CF of 6 mm length, 7 µm diameter, surface modified with polyester compatible coating material was purchased from DowAksa™, Turkey (tensile strength: 4200 MPa, tensile modulus: 240 GPa, elongation: %1.8, density: 1.76 g/cm^3). GF of 4.5 mm length and 13 µm diameter was purchased from Cam Elyaf A.S., Turkey (tensile strength: 3400–3700 MPa, tensile modulus: 72–77 GPa, elongation: %3.3–3.8, density: 2.52–2.6 g/cm^3). BF of 6 mm length and 9 µm diameter was purchased from Tila Kompozit, Turkey (tensile strength: 4840 MPa, tensile modulus: 89 GPa, elongation: %3.15, density: 2.8 g/cm^3). hBN (Density: 2.3 g/cm^3, purity: %99.97, particle size: 50–120 nm, form: powder) was supplied by BORTEK® Boron Technologies and Mechatronic Inc. (Turkey). (3-aminopropyl) tri-ethoxysilane (APTES) (molecular weight: 221.37 g/mol, purity: 98%, density: 0.948 g/mL) was purchased from Alfa Aesar and used as the silane coupling agent.

Silanization of hBN

The surface of hBN was functionalized with APTES coupling agent. For this purpose, hBN nanoparticles were dispersed in 100 ml of ethanol–distilled water solution using an ultrasonic homogenizer to obtain a stable suspension system, then the solution was mixed up with 1 ml silane and was stirred at 75 °C for 1 h. The obtained solution was washed with ethanol to remove the remaining silane around the hBN particles. The product was then dried at ambient temperature for 24 h followed by 12 h at 80 °C in a vacuum oven.

Composite preparation

TPEE was dried under vacuum in the oven at 110 °C for 3 h to evaporate moisture. Compounds containing hBN, CF, GF, BF and TPEE constituents in varying proportions by weight were compounded in a lab-scale microcompounder (DSM-Xplore, The Netherlands) at 245 °C and at a rotor speed of 100 rpm. The mixing time for all samples in the microcompounder was adjusted to 3 min. The weight ratios of the samples are detailed in Table 1.

Following the compounding process, the test specimens were produced in a laboratory-scale injection molder (DSM-Xplore, The Netherlands) with the fixed molding conditions of a barrel temperature of 245 °C, a mold temperature of 45 °C and 10 bar injection pressure.

Characterization of composites

The adhesive wear tests were conducted at ambient temperature with a standard modular pin-on-disk tribometer (Nanovea) to determine the coefficient of friction (COF) curves for the test specimens. During testing, the sample was located onto a rotational disk, and the friction radius was fixed at 5 mm, the contact load was fixed at 20 N, the sliding distance was fixed at 150 m, and the disk rotational rate was fixed at 100 rpm. The COF between the ceramic ball with a radius of 3 mm and test samples, each formulated differently, was measured and graphed throughout the entire experiment.

The tensile tests were carried out at ambient temperature at a crosshead rate of 5 mm/min with the use of a tensile tester (Shimadzu AG-X) in compliance with the ISO 527/2-5A standard. The tensile strength of each sample was recorded, and a minimum of five samples from each formulation were tested to calculate averages.

Table 1 Sample code names and composition ratios

No	Sample code	TPEE	CF	GF	BF	hBN
1	TPEE	100	0	0	0	0
2	TPEE-10hBN	90	0	0	0	10
3	TPE-CF	90	10	0	0	0
4	CF-1hBN	89	10	0	0	1
5	CF-5hBN	85	10	0	0	5
6	CF-10hBN	80	10	0	0	10
7	TPE-GF	90	0	10	0	0
8	GF-1hBN	89	0	10	0	1
9	GF-5hBN	85	0	10	0	5
10	GF-10hBN	80	0	10	0	10
11	TPE-BF	90	0	0	10	0
12	BF-1hBN	89	0	0	10	1
13	BF-5hBN	85	0	0	10	5
14	BF-10hBN	80	0	0	10	10

Three-point bending tests were carried out using a tensile tester (Instron 4411) in accordance with ISO-178 at a bending rate of 2 mm/min. Flexural stress at yield data was obtained from the test samples, and a minimum of five samples of each formulation were tested to calculate the average.

The temperature of melting (T_m) and the enthalpy of melting (ΔH_m) of the samples were analyzed by differential scanning calorimetry (DSC, TA Instruments-Q200). Thermal scans were performed between 25 °C and 250 °C with a scanning rate of 5 °C/min under a nitrogen environment. Relative degree of crystallinity $(X_c)_{rel}$ of the samples was calculated based on the DSC data by using the following equation:

$$(X_c)_{rel} = \left[\frac{(\Delta H_m - \Delta H_c)}{\Delta H_m^0 \times (1 - w)} \right] \quad (1)$$

wherein w represents the ratio by weight of reinforcements/fillers of each composition of the samples, and ΔH_m^0 (J/g) represents the enthalpy of melting of the raw TPEE which is obtained from DSC analysis.

Thermal stability of the samples was investigated using thermogravimetric analysis (TGA, TA Instruments-Q500) with a heating rate of 10 °C/min from the ambient temperature up to 600 °C under a nitrogen atmosphere. Weight loss (%) as a function of temperature was recorded.

Scanning electron microscopy (SEM, JEOL-JCM 6000) was used to examine the morphology of the samples. The SEM analysis was performed on the samples that were collected from the fractured surfaces after the tensile test. Specimens were gold sputter-coated prior to morphologic analysis.

Results and discussion

Adhesive wear test

Figure 1 shows the plots of COF versus sliding distance for TPEE composites containing CF, GF, BF and hBN. Average COF values are also shown in Table 2.

Figure 1a demonstrates the effects of the addition of 10 wt% CF and 1, 5 and 10 wt% hBN to neat TPEE on the COF. Figure 1a and Table 2 indicate that the COF reduced significantly with the addition of only CF and only 10 wt% hBN to TPEE. These results are expected because, as reported in the literature, in fiber-reinforced polymer matrix composites, the abrasive ball contacts with both the fiber and the polymer, reducing the ball/polymer contact area and causing fiber wear. Therefore, the fiber, which is more rigid when compared to the polymer, protects the polymer matrix from adhesive wear to a certain extent. Furthermore, as reported by the literature, due to its layer structure and the ability of the layers to slip on top of one another, hBN provides excellent solid lubricity and can maintain this solid lubricity up to 1200 °C under oxidative conditions. In addition, hBN with excellent thermal conductivity can effectively transfer and dissipate frictional heat to the sliding contact surface and prevent the softening of the polymer matrix to a certain extent,

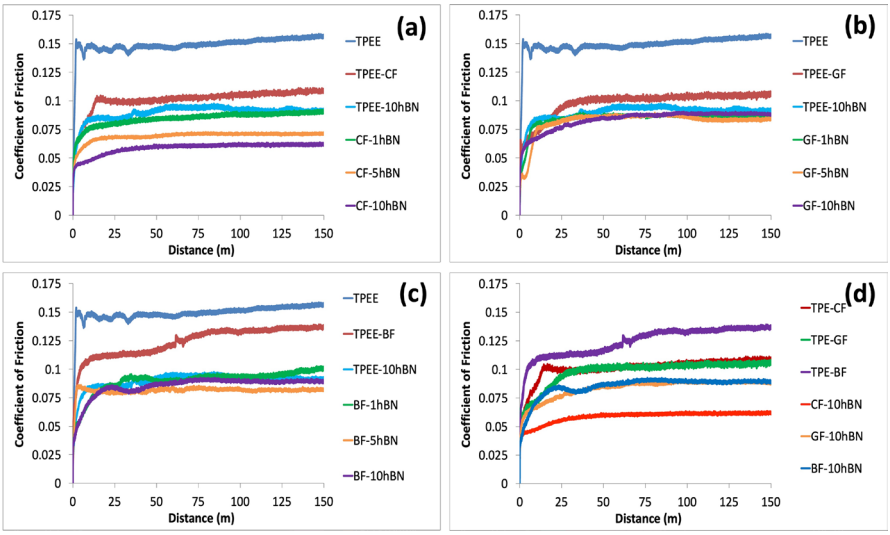

Fig. 1 Coefficient of friction curves of the test specimens

Table 2 Average results of the coefficient of friction of the samples

Material code	Average coefficient of friction (COF)
TPEE	0.121 ± 0.003
TPEE-10hBN	0.082 ± 0.010
TPEE-CF	0.101 ± 0.001
CF-1hBN	0.078 ± 0.009
CF-5hBN	0.067 ± 0.003
CF-10hBN	0.059 ± 0.005
TPE-GF	0.090 ± 0.012
GF-1hBN	0.085 ± 0.001
GF-5hBN	0.075 ± 0.016
GF-10hBN	0.072 ± 0.016
TPE-BF	0.112 ± 0.018
BF-1hBN	0.099 ± 0.008
BF-5hBN	0.088 ± 0.006
BF-10hBN	0.085 ± 0.004

thus increasing the adhesive wear resistance of composites [22, 24, 26]. For these reasons, it can be said that the addition of only CF and only hBN to neat TPEE significantly reduced the COF value and correspondingly improved the adhesive wear resistance.

However, the most important result that can be seen from Fig. 1a and Table 2 is that the COF decreases significantly both by adding hBN to the CF-reinforced TPEE matrix composite and by increasing the amount of hBN. In addition, hybrid

reinforced composites exhibited significantly lower COF than CF-only and hBN-only composites, with the lowest COF being achieved in hybrid reinforced composites containing 10 wt% hBN. When the COF curves of the hybrid reinforced composites are compared with the COF curves of the composite containing only CF and the composite containing only 10 wt% hBN, it can be seen that the simultaneous use of CF and hBN results in a hybrid effect. This hybrid effect is a result of both the dispersive effect of CF on the hBN layers and the more homogeneously dispersed hBNs in the matrix, which settle at the matrix–fiber interface and increase the interface area there, allowing more load to be transferred from the matrix to the fibers and thus allowing the fibers to carry more load without detaching from the matrix. Therefore, hBNs, which are more homogeneously dispersed in the matrix, not only perform their lubrication functions more effectively, but also help to increase the amount of load transfer from the matrix to the fiber by increasing the fiber/matrix interface area. In conclusion, it can be said that improving the dispersion of hBNs in the polymer matrix and also positioning more hBNs at the fiber/matrix interface is a good method to reduce COF and improve the adhesive wear resistance of hybrid reinforced composites [27–29].

In addition to all of the points above, it can be said that the silanization process applied to the hBN surface also contributes to increasing the interaction of hBN with both the TPEE and CF surface, as it increases the surface functionality of hBN, such that the –OH groups in the silanol molecule formed during the hydrolysis process of APTES were involved in a hydrogen bonding interaction with nitrogen atoms of the hBN surface, and as a result, the coupling of the silane molecule to the hBN surface was ensured [30]. On the other hand, the other functional end group of the silane molecule containing $–NH_2$ group tends to react to carboxyl end groups on both TPEE and CF surface [31]. This is because, as mentioned above, this study used a type of CF whose surface was modified with a coating material compatible with polyesters. As a result, it can be said that this improves the interaction of hBN with both TPEE and CF surface, thus ensuring homogeneous dispersion of hBN particles in both TPEE matrix and improving the fiber/matrix interface interaction by better positioning of hBN particles on the CF surface. Thus, it can be concluded that the functionalization of the hBN surface by the silanization process contributes to the hybrid effect.

The graph showing the effect of the addition of 10 wt% GF and 1, 5 and 10 wt% hBN to neat TPEE on the COF of TPEE is given in Fig. 1b. As can be seen in Fig. 1b and Table 2, the COF decreased with the addition of only GF and only 10 wt% hBN to TPEE. In addition, the COF decreased both by adding hBN to the GF-reinforced TPEE matrix composite and by increasing the amount of hBN, with the lowest COF being achieved in hybrid reinforced composites containing 10 wt% hBN. However, it is important to note that there is not a significant decrease between the COF of the sample type containing only 10 wt% hBN and the COF of the hybrid reinforced sample types as much as there is for the CF fiber type. Therefore, it can be interpreted that this slight decrease in COF values of hybrid reinforced composites is only due to the effect of GF to improve the homogeneous dispersion of hBN in the TPEE matrix, but the hybrid reinforcement does not contribute to the improvement of the fiber/matrix interface interaction for the GF fiber type.

Figure 1c and Table 2 show that when BF is used as the fiber type and hBN is added to the BF containing composites, the COF is reduced, i.e., the wear resistance of the composites is improved, and the lowest COF is achieved in hybrid reinforced composites containing 10 wt% hBN. However, the situation that occurred in the GF fiber type also occurred in the BF fiber type. There is no significant decrease between the COF of the sample type containing only 10 wt% hBN and the COF of the hybrid reinforced sample types as much as in the CF fiber type. Therefore, it can be interpreted that this slight decrease in COF values of hybrid reinforced composites is only due to the effect of BF to improve the homogeneous dispersion of hBN in the TPEE matrix, but the hybrid reinforcement does not contribute to the improvement of the fiber/matrix interface interaction for the BF fiber type. However, considering that BF is a fiber type that can be produced at a lower cost and with a simple production process compared to CF and GF fiber types, the improvement in wear resistance of TPEE, both when used alone and when used simultaneously with hBN, shows that BF is a positive alternative to other fiber types, especially that of GF.

Figure 1d shows a comparison of the sample types that gave the best wear resistance results. In addition, Fig. 2 shows SEM images of the adhesive wear surfaces of the sample types with the maximum and minimum COF values for comparison.

From Fig. 1d and Table 2, it can be concluded that the 10 wt% hBN and CF hybrid reinforced composite had the lowest COF and therefore the maximum wear resistance among all the sample types. In fact, as far as is known from the literature,

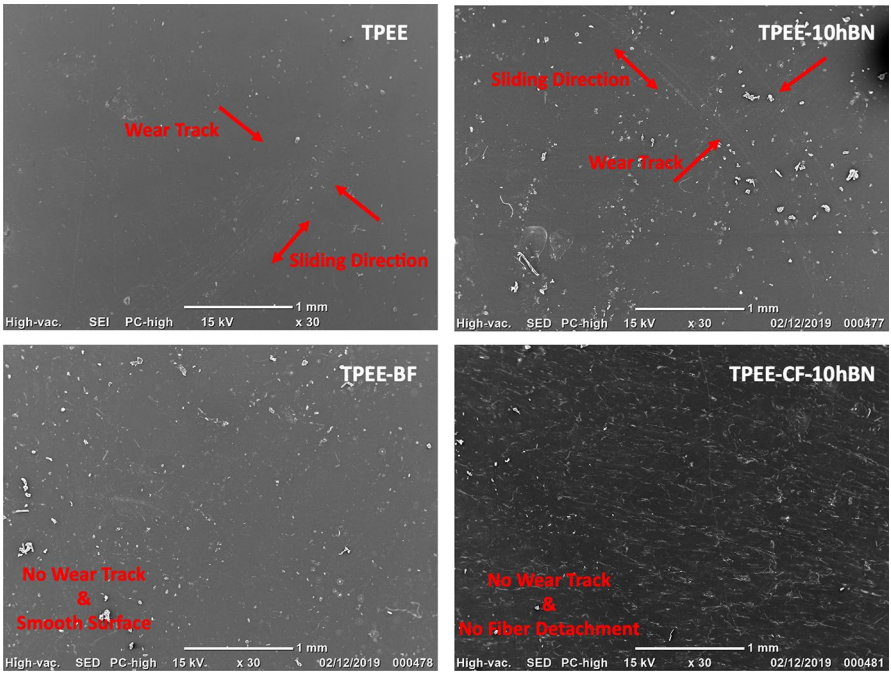

Fig. 2 SEM images of the adhesive wear surfaces of the samples

in short fiber-reinforced composites, at some point during wear, the fiber separates from the matrix, creating a three-body abrasive effect and increasing the wear. In such a case, the mechanical properties of the reinforcing material are inversely proportional to the wear resistance of the material. In other words, the higher the mechanical properties of the detached fiber, the greater the three-body abrasive effect caused by its detachment during wear [29, 32, 33]. However, it is believed that this did not happen in our study because the interface interaction between the CF and TPEE matrix was good. Thus, the abrasive ball remained in contact with the CFs embedded in the matrix throughout the wear, and therefore CF, the fiber type with the best mechanical properties, provided the lowest COF curve. This can also be seen in the SEM images shown in Fig. 2, such that CFs, which help to maintain the integrity of the structure by remaining in the matrix instead of detaching from it during wear, are visible in the SEM image. Both the graphs and the table show that the simultaneous addition of hBN and fiber produces the most effective hybrid effect in CF-reinforced composites. In fact, there is no significant decrease in COF values by adding hBN, especially in the GF-reinforced composites, while there is a significant decrease in COF by adding hBN in the CF-reinforced composite. It can be inferred that the simultaneous use of fiber and hBN only improves the dispersion of hBN in the matrix in GF and BF fiber types, but in CF fiber type it also contributes to the fiber/matrix interface interaction due to the reaction tendency between silanized hBN and CF surfaces.

Tensile test

Figure 3 shows the graph of the change in tensile strength value for TPEE composites containing hBN, CF, GF and BF.

It can be seen from Fig. 3 that the tensile strength value increased when only CF, GF and BF fiber types and only 10 wt% hBN particles were added to TPEE. In

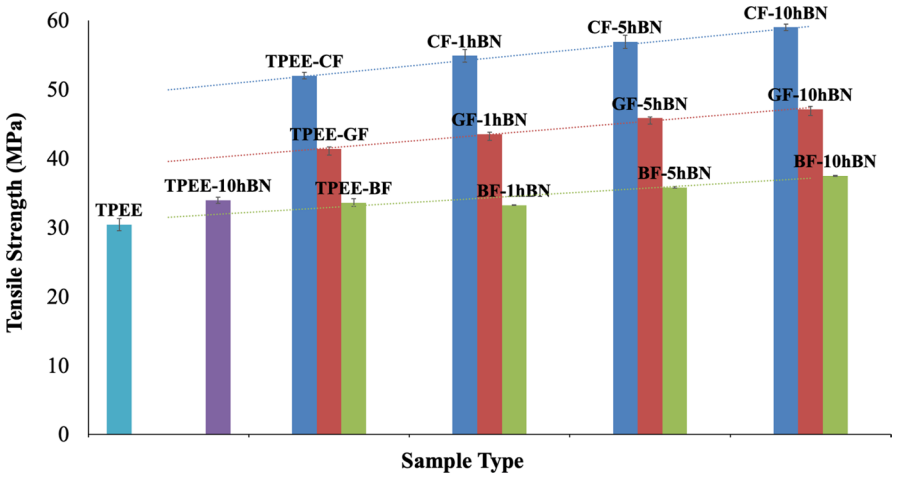

Fig. 3 Tensile strength values of specimens

addition, tensile strength increased both by adding hBN to the CF-, GF- and BF-reinforced TPEE matrix composites and by increasing the amount of hBN, such that hybrid reinforced composites exhibited higher tensile strength than only CF, GF and BF fiber types and only hBN particle-reinforced composites and the maximum tensile strength is achieved hybrid reinforced composites containing 10 wt% hBN for all fiber types.

One of the most important results to be inferred from Fig. 3 is the rate of improvement of the tensile strength values obtained for hybrid reinforced composites for each fiber type, such that adding 10 wt% hBN to CF- and GF-reinforced composites resulted in an improvement in tensile strength of approximately 14%, while by adding 10 wt% hBN to BF-reinforced composites resulted in an improvement in tensile strength of approximately 11%. As known from the literature, the improvement of the mechanical properties of a nanocomposite depends largely on the effective dispersion of the reinforcements and the interaction between the phases [26, 34]. Therefore, an important conclusion that can be drawn is that the good particle–matrix interface interaction in nanoparticle-reinforced composites and the homogeneous dispersion of the particles in the matrix have a significant role on the tensile strength property. This is because the improved interface interaction between the nanoparticles and the matrix allows for the effective transfer of stress during mechanical loading. In the present study, the tendency of hBN nanoparticles made more reactive by the surface silanization process to react with carboxyl end groups in the TPEE matrix contributed to the homogeneous dispersion of hBN particles in the TPEE matrix without agglomeration. As a result, a portion of the load applied during the tensile test was transferred to the hBN particles oriented in the plane of the tensile axis thanks to good particle–matrix interface interaction and was absorbed by the strong covalent bonds between the boron and nitrogen atoms that make up these particles. Moreover, the hBN nanoparticles homogeneously dispersed in the TPEE matrix limited the crack propagation due to the applied load. As a consequence of all these effects, the tensile strength of the material improved [27, 35]. Moreover, the improvement in tensile strength obtained with the simultaneous use of hBN particles, whose interaction with the matrix is increased by the functionalization of their surface, with the fibers also shows the positive effect of the fibers on the homogeneous dispersion of the hBN particles in the TPEE matrix.

Furthermore, when comparing the tensile strength values of hybrid reinforced composites based on fiber type, it can be said that CF-reinforced hybrid composites have the maximum tensile strength value among all specimen types and all hBN weight ratios. This high performance of the CF fiber type compared to other fiber types can be interpreted as a result of both its specific superior mechanical properties and the high quality of the interface interaction between CF and TPEE matrix material. This good interaction can be attributed to both the modifying of the CF surface with a coating material compatible with polyesters and, as mentioned above, the positioning of the surface-silanated hBN particles at the fiber/matrix interface due to their susceptibility to react with carboxyl groups [26], such that, as can be seen from the SEM images in Fig. 4, the carbon fibers are embedded in the TPEE matrix, there are TPEE residues on the surface of the fibers, and no voids are observed between the fibers and the matrix. On the other hand, there are some TPEE

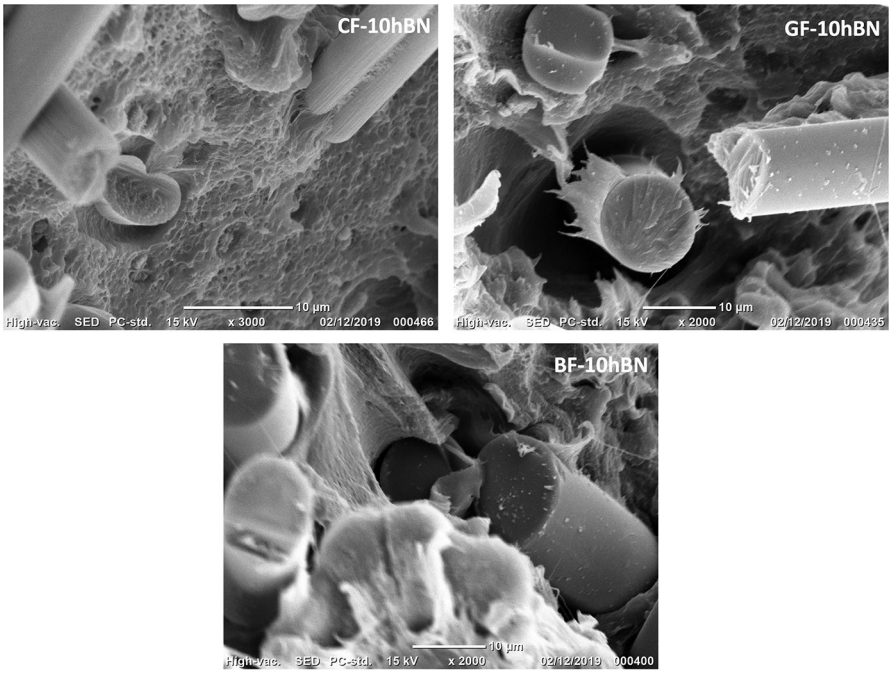

Fig. 4 SEM images of tensile fracture surfaces of samples

residues on the surfaces of GF and BF fiber types, but it is also observed that there are still significant gaps at the fiber/matrix interface.

Three-point bending test

The graph showing the changes in flexure stress at yield for the TPEE composites containing hBN, CF, GF and BF is shown in Fig. 5.

Figure 5 shows that the flexure stress at yield increased with the addition of only CF, GF and BF fiber types and only 10 wt% hBN particles to TPEE. In addition, the flexure stress at yield increased both by adding hBN to the CF-, GF- and BF-reinforced TPEE matrix composites and by increasing the amount of hBN. Thus, the hybrid reinforced composites exhibited higher flexure stress than the CF, GF, BF alone and the hBN alone reinforced composites, and the maximum flexure stress is achieved by the hybrid reinforced composites containing 10 wt% hBN for all fiber types.

The flexure test is a method of characterizing the performance of materials exposed to simple beam loading and the flexural properties obtained from this test provide information about the behavior of the material in bending. The flexural strength of a fiber-reinforced composite can be generally defined as the maximum stress at the outermost lift. Three-point bending is the most commonly used flexural test for polymers. The literature review shows that there are a number of material

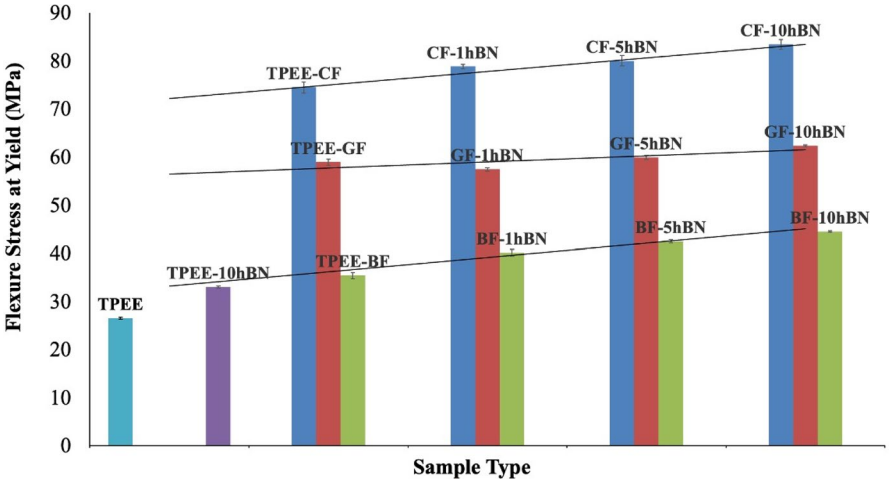

Fig. 5 Flexure stress at yield values of specimens

properties on which the flexural properties of polymer composites depend. These material properties are the interface interaction between the reinforcement and the matrix, the strength of the reinforcement, the physical properties of the reinforcement, and the amount of reinforcement [2, 36–40].

The amount of reinforcement is an important factor in flexural strength because flexural strength is determined by the capability of the composite to resist flexural loads, and increasing the amount of reinforcement allows for greater resistance to flexural loads. Evaluating Fig. 5 from this point of view, it can be concluded that the increase in flexural stress with both the addition of fiber to neat TPEE and the addition of hBN at increasing weight ratios to fiber-reinforced TPEE is due to the increase in load carrying capacity of TPEE compared to its unreinforced state.

The physical properties of the reinforcement including density, length and strength are also important factors in flexural strength. Low density reinforcements are generally preferred due to their higher bending capability. Also, the length of the fiber must not be less than the critical length as this will adversely affect the stress transfer capability between the fiber and the matrix. On the other hand, the higher the individual strength of the reinforcing material, the higher its ability to carry the load transferred from the matrix during bending. Therefore, as shown in Fig. 5, the observation of the maximum flexural stresses in CF-reinforced composites is attributed to the fact that CF has both the highest strength and the lowest density compared to other fiber types. In addition, as a result of the high interface interaction between CF and TPEE matrix, the fibers break less during the composite manufacturing process and their length remains closer to the critical fiber length, allowing CF to perform its reinforcing task more effectively than GF and BF fiber types [41].

The interface interaction between the matrix and the reinforcement is important because higher interface adhesion facilitates the transfer of stress from the matrix to the reinforcement and improves flexural strength. In addition, when the fiber/matrix interface interaction is strong, the fibers break less during composite production and

thus their final length is closer to the critical fiber length, which increases their reinforcing efficiency. On the other hand, depending on the type of filler, surface unmodified and hydrophilic nanoparticles may not be uniformly dispersed in the matrix phase and may agglomerate. This causes the stress in the matrix to be concentrated at certain points in the matrix phase and cracks at these points can easily propagate to the non-reinforced parts of the matrix. This is a major cause of crack propagation leading to a reduction in flexural strength and matrix fracture. Surface modification of nanoparticles can effectively improve their dispersion by polarizing them. The homogeneous dispersion of nanoparticles prevents the propagation of cracks in the composite structure and provides a significant improvement in flexural strength properties [40]. As shown in Fig. 5, the flexural stress increased with the addition of silane-modified hBN to both pure TPEE and fiber-reinforced TPEE matrix composites. This increase continued even with increasing hBN loading. From this point of view, it can be said that hBN is homogeneously dispersed in composite structures containing all fiber types by becoming polar as a result of surface modification, thus acting both as a nano-reinforcement in the TPEE matrix and as a modifier that increases the interface area by positioning itself at the fiber/matrix interface, thus assuming the functions of both load carrying and load transferring.

Differential scanning calorimetry analysis

The variation of T_m and X_c values of TPEE with the addition of CF, GF, BF and hBN was evaluated by DSC analysis, and the resulting data are listed in Table 3.

Table 3 shows that the T_m of neat TPEE did not alter by adding CF, GF and BF fiber types alone and by adding 10 wt% hBN alone. Table 3 also shows that the X_c value of neat TPEE was significantly reduced by adding CF, GF and BF fiber types alone and by adding 10 wt% hBN alone. Furthermore, this decrease in X_c value continued to increase both by adding hBN to the fiber-reinforced composites and by

Table 3 Results of the DSC analysis of samples

Material code	T_m (°C)	X_c (%)$_{rel}$
TPEE	218.22	100.00
TPEE-10hBN	218.92	88.70
TPEE-CF	218.74	95.32
CF-1hBN	218.16	94.50
CF-5hBN	218.62	88.53
CF-10hBN	218.69	82.65
TPEE-GF	219.25	99.23
GF-1hBN	218.61	94.09
GF-5hBN	218.61	91.56
GF-10hBN	218.59	87.05
TPEE-BF	218.61	99.23
BF-1hBN	219.18	90.60
BF-5hBN	218.76	88.02
BF-10hBN	218.81	86.25

increasing the amount of hBN. This decrease in X_c value by adding CF, GF, BF, hBN and by increasing the amount of hBN can be explained based on the free volume and the interaction factors between the reinforcement materials and the TPEE, such that it can be concluded that with the inclusion of only fibers or only hBN, these materials were homogeneously dispersed in the matrix and intercalated between the TPEE chains, thus making it difficult for the TPEE chains to get close to each other to crystallize, thus reducing the relative degree of crystallinity of the TPEE matrix. In other words, these reinforcing materials dominated a portion of the free volume in the TPEE matrix and restricted the molecular motions of the polymer chains, causing a reduction in X_c by restricting the chains from easily crystallizing. In addition, while X_c was 88.7% in composites containing only 10 wt% hBN, it decreased below this value in hybrid reinforced composites containing 10 wt% hBN, again demonstrating the synergistic effect between fiber types and hBN and the contribution of fibers in the structure to the homogeneous dispersion of nanoparticles [22, 27].

On the other hand, when comparing the decrease in X_c value based on the fiber type, it can be seen that the largest decrease occurs in CF-reinforced composites containing 10 wt% hBN and decreases to 82.65%. The fact that the maximum decrease occurs in the case where CF fiber type is used can be interpreted as the fact that when hBN is used simultaneously with CF, it not only acts as a reinforcement by dispersing in the matrix, but also improves the interface interaction here by positioning itself at the fiber/matrix interface, thus reducing the mobility of carbon fibers whose interaction with the matrix increases, and thus preventing the polymer chains of the matrix from coming closer to each other and preventing crystallization [22, 27]. Therefore, this result can be interpreted as the best interface interaction between fiber and matrix will result in the lowest X_c value. This is because the CF-reinforced composite containing 10 wt% hBN, which has the lowest X_c value among the X_c values shown in Table 3, also exhibited the best mechanical and tribological performance.

Thermogravimetric analysis

TGA is a thermal analysis method that can be used to assess the thermal stability of materials. In this study, in order to evaluate the thermal stability of the materials, the initial thermal degradation temperature at 10% weight loss ($T_{10\%}$) and the degradation temperature at 50% weight loss ($T_{50\%}$) were determined through TGA thermograms, and these values are listed in Table 4.

Table 4 shows that the initial decomposition temperature of neat TPEE ($T_{10\%}$) was significantly increased by adding CF, GF and BF fiber types alone and by adding 10 wt% hBN alone. Furthermore, it is seen that this increase continues both by adding hBN to the fiber-reinforced composites and by increasing the amount of hBN. So much so that the addition of 10 wt% hBN alone to neat TPEE increased the $T_{10\%}$ temperature by about 7 °C, while the addition of any type of fiber alone increased the $T_{10\%}$ temperature by about 8 °C, and the simultaneous addition of fiber and hBN increased this increase up to 11 °C. Therefore, it appears that it is not the type of fiber used, but the simultaneous use of fiber and hBN that has a major effect on the

Table 4 TGA results of samples

Material code	$T_{10\%}$ (°C)	$T_{50\%}$ (°C)
TPEE	364.37	389.98
TPEE-10hBN	371.53	398.13
TPE-CF	372.30	398.43
CF-1hBN	375.72	401.09
CF-5hBN	375.01	401.77
CF-10hBN	375.30	403.04
TPE-GF	373.93	399.65
GF-1hBN	373.50	399.28
GF-5hBN	375.34	401.83
GF-10hBN	375.25	402.64
TPE-BF	372.60	398.69
BF-1hBN	374.92	400.72
BF-5hBN	374.70	401.33
BF-10hBN	374.48	402.61

degradation temperature. Thus, it can be concluded that both the addition of fiber to the neat polymer and the simultaneous addition of fiber and hBN increase the initial thermal degradation temperature of TPEE and thus improve its thermal stability.

Similarly, when examining the $T_{50\%}$ temperatures shown in Table 4, it can be seen that the $T_{50\%}$ of neat TPEE was significantly increased by adding CF, GF and BF fiber types alone and by adding 10 wt% hBN alone. Furthermore, this increase continues both by adding hBN to the fiber-reinforced composites and by increasing the amount of hBN. So much so that the addition of 10 wt% hBN alone to neat TPEE increased the $T_{50\%}$ temperature by about 9 °C, while the addition of any type of fiber alone increased the $T_{50\%}$ temperature by about 10 °C, and the simultaneous addition of fiber and hBN increased this increase up to 13 °C. Although the maximum increase in $T_{50\%}$ temperature is observed in the CF-reinforced composite containing 10 wt% hBN, the effect of the simultaneous addition of fiber and hBN to neat TPEE on thermal stability cannot be ignored.

This increase in $T_{10\%}$ and $T_{50\%}$ temperatures can be explained by the fact that CF, GF, BF and hBN have higher thermal conductivity and specific heat capacity properties than neat TPEE. Therefore, when thermal energy is applied to composites, these reinforcing materials can absorb more heat due to their higher heat capacity than the matrix material and distribute the absorbed heat more easily within the structure due to their higher thermal conductivity than the matrix material, thus contributing to the maintenance of the thermal stability of the composite. It is also known from the literature that layered fillers such as hBN, due to their layered structure, can act as heat sinks during the degradation process of the composite to which they are added, trapping the degradation products between the layers and thus delaying the degradation process of the composite, i.e., acting as a physical barrier [22, 27]. In this study, the increase in degradation temperature with increasing hBN content in hybrid reinforced composites is attributed to both the high thermal properties of hBN and its layered structure, which has the ability to retard degradation. Besides, the fact that

the maximum degradation temperature was determined in CF-reinforced hybrid composites containing 10 wt% hBN confirms a previous result and proves once again the synergistic effect that occurs when hBN and CF are used together.

Conclusions

In the present study, the influence of hexagonal boron nitride (hBN) addition at different weight ratios to thermoplastic polyester elastomer (TPEE) matrix composites reinforced with three different fiber types, namely carbon fiber (CF), glass fiber (GF) and basalt fiber (BF), on the thermal, tribological and mechanical properties of the composites was studied.

Adhesive wear test results revealed that the COF value decreased significantly with the simultaneous addition of hBN and CF to TPEE, and with increasing the amount of hBN, the lowest COF was obtained in composites containing 10 wt% of hBN and CF simultaneously. This result was attributed to the more homogeneous dispersion of the surface-silanated functionalized hBN in the TPEE matrix when added simultaneously with the fibers and also to its positioning at the fiber/matrix interface due to the chemical interaction with the surface of the CF fiber type compared to other fiber types. The carbon fibers with high interaction with the TPEE matrix remained in the matrix and came into contact with the abrasive ball rather than detaching from the matrix during wear process, helping to maintain the integrity of the matrix and making the matrix less affected by adhesive wear. In addition, hBN particles in the form of platelets, which are more homogeneously dispersed in the matrix when used simultaneously with the fiber, also ensured that the load applied during adhesive wear was absorbed in their structures in the form of sliding between the layers, again helping to protect the integrity of the matrix.

Similar results were obtained in tensile and three-point bending tests. In fact, the maximum tensile strength was obtained in composites containing 10 wt% hBN and CF simultaneously. This result was attributed to both the higher specific strength of CF compared to other fiber types and the higher interaction between the CF surface and the TPEE matrix and hBN. This result was also supported by SEM images. The results of the three-point bending test showed that the flexural strength increased with both the addition of fiber to pure TPEE and the addition of hBN at increasing weight ratios to fiber-reinforced TPEE matrix composites, and the maximum flexural strength was obtained in composites containing 10 wt% hBN and CF simultaneously. This result was attributed to many factors. These factors are: the addition of reinforcement material and the increase in the load carrying ability of the material with increasing amount of reinforcement material, CF being the fiber type with the maximum strength and lowest density compared to other fiber types. In addition, due to the good interface interaction between CF and TPEE matrix, CF can exhibit its performance more effectively by remaining close to the critical fiber length due to less breakage during the composite manufacturing process, and finally, hBN particles are homogeneously dispersed in the TPEE matrix to carry the bending load applied to the matrix and prevent crack propagation.

DSC analysis results showed that the chain mobility decreased with the addition of reinforcement material to neat TPEE, resulting in a decrease in X_c. This decrease was most pronounced in composites containing 10 wt% of hBN and CF simultaneously. This result is interpreted as the interaction between hBN and CF, whereby hBN is not only homogeneously dispersed in the TPEE matrix, but also located at the fiber/matrix interface, further reducing the chain mobility of TPEE, resulting in an additional decrease in X_c. The TGA results also showed that both the addition of fibers and hBN alone and the simultaneous addition of fibers and hBN to neat TPEE improved the thermal stability of the material. This improvement was further enhanced with increasing hBN weight ratio in hybrid reinforced composites and the maximum improvement was observed in composites containing 10 wt% hBN and CF simultaneously. The increase in thermal stability, especially when hBN was used concurrently with CF, was attributed to the fact that hBN in the form of platelets can more effectively exhibit thermal degradation retardation performance when it is homogeneously dispersed in the matrix.

In conclusion, this study has shown that the addition of hBN to fiber-reinforced TPEE matrix composites, regardless of fiber type, and the increasing weight ratio of hBN improves the wear, mechanical and thermal properties of the composites and increases their performance potential in the relevant application areas. Therefore, hBN, a nano-sized platelet-shaped particle, can be used as a hybrid reinforcement to improve the properties of fiber-reinforced composites. However, when the synergistic effect of hBN when used simultaneously with fiber reinforcement was compared on the basis of fiber type, CF was found to outperform GF and BF fiber types. There are two main reasons for this finding. The first is the high specific properties of CF compared to other fiber types, and the second is its susceptibility to chemical interactions with both the TPEE matrix and the surface-silanated hBN due to its surface treatment with a polyester compatible coating material. Therefore, for these reasons, hybrid reinforced composites containing 10 wt% hBN and CF exhibit superior tribological, mechanical and thermal properties. However, it should be noted that the performance of BF is comparable to that of GF, which is the most widely used fiber in the composites industry, which means that the low cost advantage of BF may allow it to be a substitute for GF where performance requirements allow.

Acknowledgements This study was supported by The Scientific and Technological Research Council of Turkey under the 1505-University-Industry Collaboration Support Program (Project No: 5160067).

Author contributions Okan Gul, PhD, performed investigation and writing—original draft. N. Gamze Karsli, PhD, contributed to conceptualization, investigation, methodology, resources, writing—original draft, and writing—review and editing. Cihat Gul, PhD, performed investigation and writing—original draft. Ali Durmus, PhD, contributed to conceptualization, investigation, methodology, and resources. Taner Yilmaz, PhD, contributed to conceptualization, investigation, methodology, resources, and writing—review and editing.

Data availability The data supporting the findings of this study are available within the paper. Should any raw data files be needed in another format they are available from the corresponding author upon reasonable request. Source data are provided with this paper.

Declarations

Conflict of interest The authors declare no competing interests.

References

1. Bae J, Lee S, Kim BC, Cho HH, Chae DW (2013) Polyester-based thermoplastic elastomer/MWNT composites: rheological, thermal, and electrical properties. Fibers Polym 14(5):729–734. https://doi.org/10.1007/s12221-013-0729-8
2. Hemanth R, Suresha B, Sekar M (2015) Physico-mechanical behaviour of thermoplastic co-polyester elastomer/polytetrafluroethylene composite with short fibers and microfillers. J Compos Mater 49(18):2217–2229. https://doi.org/10.1177/0021998314545183
3. Sreekanth MS, Joseph S, Mhaske ST, Mahanwar PA, Bambole VA (2011) Effects of mica and fly ash concentration on the properties of polyester thermoplastic elastomer composites. J Thermoplast Compos Mater 24:317–331. https://doi.org/10.1177/0892705710389293
4. Chen J, Lv Q, Wu D, Yao X, Wang J, Li Z (2016) Nucleation of a thermoplastic polyester elastomer controlled by silica nanoparticles. Ind Eng Chem Res 55:5279–5286. https://doi.org/10.1021/acs.iecr.5b04464
5. Qiu Y, Wu D, Xie W, Wang Z, Peng S (2018) Thermoplastic polyester elastomer composites containing two types of filler particles with different dimensions: structure design and mechanical property control. Compos Struct 197:21–27. https://doi.org/10.1016/j.compstruct.2018.05.035
6. Qiu Y, Wang J, Wu D, Wang Z, Zhang M, Yao Y, Wei N (2016) Thermoplastic polyester elastomer nanocomposites filled with graphene: mechanical and viscoelastic properties. Compos Sci Technol 132:108–115. https://doi.org/10.1016/j.compscitech.2016.07.005
7. Pearson A, Liao W, Heydrich M, Kakroodi A, Hammami A, Kazemi Y, Naguib HE (2021) Role of interfacial adhesion and fiber length on the mechanical performance fiber reinforced thermoplastic elastomers. Compos Sci Technol 213:108928. https://doi.org/10.1016/j.compscitech.2021.108928
8. Corrêa RA, Nunes RCR, Franco Filho WZ (1998) Short fiber reinforced thermoplastic polyurethane elastomer composites. Polym Compos 19(2):152–155. https://doi.org/10.1002/pc.10086
9. Pesetskii SS, Shevchenko VV, Dubrovsky VV (2018) Morphology and properties of poly(ethylene terephthalate) and thermoplastic polyester elastomer blends modified in the melt by a diisocyanate chain extender and filled with a short glass fiber. J Appl Polym Sci 135:45711. https://doi.org/10.1002/app.45711
10. Shonaike GO, Matsuo T (1996) An experimental study of impregnation conditions on glass fiber reinforced thermoplastic polyester elastomer composites. J Reinf Plast Compos 15(1):16–29. https://doi.org/10.1177/073168449601500102
11. Abdo D, Gleadall A, Silberschmidt VV (2019) Damage and damping of short-glass-fibre-reinforced PBT composites under dynamic conditions: effect of matrix behaviour. Compos Struct 226:111286. https://doi.org/10.1016/j.compstruct.2019.111286
12. Abdo D, Gleadall A, Silberschmidt VV (2019) Failure behaviour of short-fibre-reinforced PBT composites: effect of strain rate. Eng Fail Anal 105:466–476. https://doi.org/10.1016/j.engfailanal.2019.07.028
13. Iyer S, Detwiler A, Patel S, Schiraldi DA (2006) Control of coefficient of thermal expansion in elastomers using boron nitride. J Appl Polym Sci 102:5153–5161. https://doi.org/10.1002/app.24705
14. Pandey N, Tewari C, Dhali S, Bohra BS, Rana S, Mehta SPS, Singhal S, Chaurasia A, Sahoo NG (2021) Effect of graphene oxide on the mechanical and thermal properties of graphene oxide/hytrel nanocomposites. J Thermoplast Compos Mater 34(1):55–67. https://doi.org/10.1177/0892705719838010
15. Aso O, Eguiazábal JI, Nazábal J (2007) The influence of surface modification on the structure and properties of a nanosilica filled thermoplastic elastomer. Compos Sci Technol 67:2854–2863. https://doi.org/10.1016/j.compscitech.2007.01.021
16. Shonaike GO, Matsuo T (1995) Fabrication and mechanical properties of glass fibre reinforced thermoplastic elastomer composites. Compos Struct 32:445–451. https://doi.org/10.1016/0263-8223(95)00076-3

17. Almushaikeh AM, Alaswad SO, Alsuhybani MS, AlOtaibi BM, Alarifi IM, Alqahtani NB, Aldosari SM, Alsaleh SS, Haidyrah AS, Alolyan AA, Alshammari BA (2023) Manufacturing of carbon fiber reinforced thermoplastics and its recovery of carbon fiber: a review. Polym Testing 122:108029. https://doi.org/10.1016/j.polymertesting.2023.108029
18. Suresha B, Hemanth G, Hemanth R, Lalla NP (2020) Role of graphene nanoplatelets and carbon fiber on mechanical properties of PA66/thermoplastic copolyester elastomer composites. Mater Res Express 7:015325. https://doi.org/10.1088/2053-1591/ab648d
19. Alshammari BA, Alsuhybani MS, Almushaikeh AM, Alotaibi BM, Alenad AM, Alqahtani NB, Alharbi AG (2021) Comprehensive review of the properties and modifications of carbon fiber-reinforced thermoplastic composites. Polymers-Basel 13(15):2474. https://doi.org/10.3390/polym13152474
20. Fiore V, Scalici T, Di Bella G, Valenza A (2015) A review on basalt fibre and its composites. Compos B Eng 74:74–94. https://doi.org/10.1016/j.compositesb.2014.12.034
21. Kizil A, Dincer U, Yilmaz S, Gul O, Karsli NG, Yilmaz T (2023) Investigation of the effect of zeolite, bentonite, and basalt fiber as natural reinforcing materials on the material properties of PPS and CF-reinforced PPS. Polym Eng Sci 63(4):1314–1322. https://doi.org/10.1002/pen.26285
22. Aslan C, Karsli NG (2024) Investigation of the synergetic effect of hybrid fillers of hexagonal boron nitride, graphene nanoplatelets and short basalt fibers for improved properties of polyphenylene sulfide composites. Polym Bull 81:4969–4992. https://doi.org/10.1007/s00289-023-04940-0
23. Zheng Z, Cox MC, Li B (2018) Surface modification of hexagonal boron nitride nanomaterials: a review. J Mater Sci 53:66–99. https://doi.org/10.1007/s10853-017-1472-0
24. Khalaj M, Golkhatmi SZ, Alem SAA, Baghchesaraee K, Azar MH, Angizi S (2020) Recent progress in the study of thermal properties and tribological behaviors of hexagonal boron nitride-reinforced composites. J Compos Sci 4:116. https://doi.org/10.3390/jcs4030116
25. Ribeiro H, Trigueiro JPC, Owuor PS, Machado LD, Woellner CF, Pedrotti JJ, Jaques YM, Kosolwattana S, Chipara A, Silva WM, Silva CJR, Galvão DS, Chopra N, Odeh IN, Tiwary CS, Silva GG, Ajayan PM (2018) Hybrid 2D nanostructures for mechanical reinforcement and thermal conductivity enhancement in polymer composites. Compos Sci Technol 159:103–110. https://doi.org/10.1016/j.compscitech.2018.01.032
26. Yang F, Li J, Han S, Ma N, Li Q, Liu D, Sui G (2023) Wear resistant PEEK composites with great mechanical properties and high thermal conductivity synergized with carbon fibers and h-BN nanosheets. Polym Adv Technol 34:2224–2234. https://doi.org/10.1002/pat.6043
27. Karsli NG (2023) Carbon fiber reinforced poly(lactic acid) composites: investigation the effects of graphene nanoplatelet and coupling agent addition. J Elastom Plast 55(6):858. https://doi.org/10.1177/00952443231183141
28. Karsli NG, Gul O, Yilmaz T (2022) Investigation of the synergistic effect of addition the hybrid carbon fiber, graphene nanoplatelet and matrix modifier to poly(phenylene sulphide) on physical properties. Fibers Polym 23(4):1059–1067. https://doi.org/10.1007/s12221-022-4215-z
29. Harsha AP, Tewari US (2003) The effect of fibre reinforcement and solid lubricants on abrasive wear behavior of polyetheretherketone composites. J Reinf Plast Compos 22(8):751–767. https://doi.org/10.1177/0731684403022008005
30. Tsuji Y, Kitamura Y, Someya M, Takano T, Yaginuma M, Nakanishi K, Yoshizawa K (2019) Adhesion of epoxy resin with hexagonal boron nitride and graphite. ACS Omega 4(3):4491–4504. https://doi.org/10.1021/acsomega.9b00129
31. Georgiopoulos P, Kontou E, Georgousis G (2018) Effect of silane treatment loading on the flexural properties of PLA/flax unidirectional composites. Compos Commun 10:6–10. https://doi.org/10.1016/j.coco.2018.05.002
32. Karsli NG, Demirkol S, Yilmaz T (2016) Thermal aging and reinforcement type effects on the tribological, thermal, thermomechanical, physical and morphological properties of poly(ether ether ketone) composites. Compos B Eng 88:253–263. https://doi.org/10.1016/j.compositesb.2015.11.013
33. Suresha B, Kumar KNS (2009) Investigations on mechanical and two-body abrasive wear behaviour of glass/carbon fabric reinforced vinyl ester composites. Mater Design 30(6):2056. https://doi.org/10.1016/j.matdes.2008.08.038
34. Lopes MC, de Castro VG, Seara LM, Diniz VPA, Lavall RL, Silva GG (2014) Thermosetting polyurethane-multiwalled carbon nanotube composites: thermomechanical properties and nanoindentation. J Appl Polym Sci 131:41207. https://doi.org/10.1002/app.41207
35. Ribeiro H, Trigueiro JPC, Woellner CF, Pedrotti JJ, Miquita DR, Silva WM, Lopes MC, Fechine GJM, Luciano MA, Silva GG, Ajayan PM (2020) Higher thermal conductivity and mechanical

enhancements in hybrid 2D polymer nanocomposites. Polym Test 87:106510. https://doi.org/10.1016/j.polymertesting.2020.106510
36. Khan MZR, Srivastava SK, Gupta MK (2018) Tensile and flexural properties of natural fiber reinforced polymer composites: a review. J Reinf Plast Compos 37(24):1435–1480. https://doi.org/10.1177/0731684418799528
37. Asim M, Jawaid M, Abdan K, Ishak MR (2017) Effect of pineapple leaf fibre and kenaf fibre treatment on mechanical performance of phenolic hybrid composites. Fibers Polym 18(5):940–947. https://doi.org/10.1007/s12221-017-1236-0
38. Al-Mosawi AI, DrMA R, Abdullah N, Mahdi S (2013) Flexural strength of fiber reinforced composite. Int J Enhanc Res Sci Technol Eng 2(1):1–3
39. Bachtiar D, Sapuan SM, Hamdan MM (2010) Flexural properties of alkaline treated sugar palm fibre reinforced epoxy composites. Int J Automot Mech Eng (IJAME) 1:79–90. https://doi.org/10.15282/ijame.1.2010.7.0007
40. Mortazavi V, Atai M, Fathi M, Keshavarzi S, Khalighinejad N, Badrian H (2012) The effect of nanoclay filler loading on the flexural strength of fiberreinforced composites. Dent Res J 9(3):273–280
41. Karsli NG, Aytac A, Deniz V (2012) Effects of initial fiber length and fiber length distribution on the properties of carbon-fiber-reinforced-polypropylene composites. J Reinf Plast Compos 31(15):1053–1060. https://doi.org/10.1177/0731684412452678